

Mechanical characterization of single high-strength electrospun polyimide nanofibres

Fei Chen¹, Xinwen Peng¹, Tingting Li¹, Shuiliang Chen¹, Xiang-Fa Wu², Darrell H Reneker³ and Haoqing Hou^{1,4}

¹ Chemistry and Chemical Engineering College, Jiangxi Normal University, Nanchang, 330022, People's Republic of China

² Department of Engineering Mechanics, University of Nebraska–Lincoln, Lincoln, NE 68588-0526, USA

³ Department of Polymer Science, University of Akron, Akron, OH 44325, USA

E-mail: haoqing@jxnu.edu.cn (H. Q. Hou)

Received 25 September 2007, in final form 25 October 2007

Published 4 January 2008

Online at stacks.iop.org/JPhysD/41/025308

Abstract

Ultimate tensile strength and axial tensile modulus of single high-strength electrospun polyimide [poly(*p*-phenylene biphenyltetracarboximide), BPDA/PPA] nanofibres have been characterized by introducing a novel micro tensile testing method. The polyimide nanofibres with diameters of around 300 nm were produced by annealing their precursor (polyamic acid) nanofibres that were fabricated by the electrospinning technique. Experimental results of the micro tension tests show that polyimide nanofibres had an average ultimate tensile strength of 1.7 ± 0.12 GPa, axial tensile modulus of 76 ± 12 GPa and ultimate strain of $\sim 3\%$. The ultimate tensile strength and axial tensile modulus of the electrospun polyimide nanofibres in this study are among the highest ones reported in the literature to date. The precursor nanofibres with similar diameters and molecular weights had an average ultimate tensile strength of 766 ± 41 MPa, axial tensile modulus of 13 ± 0.4 GPa and ultimate strain of $\sim 43\%$. The experimental stress–strain curves obtained in this study indicate that under axial tension, the precursor (polyamic acid) nanofibres behave as linearly strain-hardening ductile material without obvious softening at final failure, while the polyimide nanofibres behave simply as brittle material with very high tensile strength and axial tensile modulus. Furthermore, by using a transmission electron microscope, detailed fractographical analysis was performed to examine the tensile failure mechanisms of the polyimide nanofibres, which include chain scission, pull-out, chain bundle breakage, etc. X-ray diffraction analysis of the highly aligned polyimide nanofibres shows the high chain alignment along the nanofibre axis that was formed in the electrospinning process and responsible for the high tensile strength and axial tensile stiffness.

(Some figures in this article are in colour only in the electronic version)

1. Introduction

Continuous nanofibres produced by the electrospinning technique represent a new class of one-dimensional (1D) nanomaterials with high surface area to volume ratio and controllable microstructures and surface morphology [1–6].

Electrospinning is a unique top-to-down nanomanufacturing process which is based on electrohydrodynamics by applying the electrical drawing force directly on the jet body. To date, over two hundred synthetic and natural fibres have been produced by electrospinning with their diameters ranging from about a nanometre to a few micrometres [7–9]. Continuous nanofibres collected in the electrospinning process can be in the form of highly porous non-woven nanofibrous mats [10–13] or

⁴ Author to whom any correspondence should be addressed.

highly aligned nanofibre films [3, 14]. So far, electrospinning has become a worldwide topic of interest due to the rapidly increasing applications in protective clothing [15], filtration [16], templates for producing metallic or polymer nanotubes [16–18], precursors for fabricating carbon nanofibres [19, 20], and nanofibre composites [21]. Furthermore, electrospun nanofibres can also be used in biomedical engineering and technologies such as medications [22, 23], scaffolds for tissue growth [24–26], drug delivery systems [27, 28], dye-sensitized solar cells [29, 30], super-hydrophobic surfaces [31, 32] and nanofibre sensors [33], etc. Near future applications of nanofibres may also include solar sails, light sails and mirrors in space and nanoelectronics [34], among others.

As a matter of fact, for electrospun nanofibres integrated in advanced nanomaterials and microstructural components, they have to bear sufficient mechanical properties to perform their targeted functionalities in the above applications. Mechanical properties of individual nanofibres also dominate their deformations, dynamics, stability, adhesion and contacts and global mechanical response of nanofibre devices and nanofibre networks [35–42]. So far, several experimental methods have been dedicated to the mechanical characterization of electrospun nanofibres in recent years. Among those, the simplest experimental method is based on the tensile testing of a nanofibrous mat on a universal testing machine [43–49]. The reliability of such a tension test greatly depends on the nanofibre diameters, alignment and effects of fibre conglutination and entanglements inside the nanofibrous mat. Furthermore, in such tests, the thickness measurement of the nanofibrous mat is still questionable. For instance, the mat thickness extracted from the sample weight per unit area and the mass density [50] of the bulk polymer material was about 7–10 times thinner than that measured by using a micrometre and with the sample sandwiched between two glass slides. Use of a thickness transducer, e.g. the CMI100 Coating Measurement (Oxford Instruments), has also revealed higher values of the sample thickness.

Recently, investigations have also been reported to characterize the axial modulus of single electrospun nanofibres by using an atomic force microscope (AFM) [51–60]. Two typical testing methods have been developed, i.e. the AFM-based uniaxial tension and three-point bending tests. In a typical uniaxial tension test, one end of the nanofibre segment is fastened on the surface of a silicon wafer by adhesive, and the other end is tethered to the AFM tip. The microscopic tensile force is exerted through the motion of the AFM tip. In the case of a micro three-point bending test, the nanofibre segment is clamped at the two ends by adhesive on the surface of a silicon wafer with periodic grooves. The transverse bending force is induced by the AFM tip at the midspan of the nanofibre segment between two neighbouring supports. As a result, the force-displacement curve can be captured in either method above, which can be further used for the axial modulus calculation. Nevertheless, the ultimate tensile strength and ultimate strain are still difficult to be determined through the AFM. Without doubt, the best way to characterize the mechanical properties of electrospun nanofibres would

be to perform a direct tension test of nanofibres. To do so, two main challenges must be faced. One is to precisely measure the nanofibre diameter which was also confronted in the testing methods mentioned earlier, and the other is to accurately capture the tensile force which is extremely low in the range of a few micronewtons to millinewtons. In a recent study, micro tension test of single electrospun fibres (polycarbolactone) has been demonstrated by using a micro tension tester (NanoBionix, MTS, USA) [61]. The diameters of the polycarbolactone fibres were above $1\ \mu\text{m}$, which are much larger than that of the nanofibres to be studied in this work.

Nevertheless, based on authors' knowledge, the ultimate tensile strength and axial tensile modulus of electrospun polymer nanofibres reported in the literature were much lower than those of their thicker counterparts obtained by conventional extrusion. The possible reasons are that the molecular chains inside an electrospun fibre are not in good alignment along the fibre axis, and the molecular weights of these polymer chains are also relatively low. Recently, significant efforts have been dedicated to enhancing the tensile strength of electrospun nanofibres. Among other findings, this paper reports our recent experimental results regarding the mechanical properties of single high-strength polyimide (BPDA/PPA) nanofibres. Polyimide nanofibres with diameters around 300 nm were produced through electrospinning home-synthesized poly(*p*-phenylene biphenyltetracarboximide) (BPDA/PPA) and annealing afterwards. The testing procedure of the single nanofibre tension test is described in detail. The tensile stress–strain curves of the polyimide nanofibres and their precursor (polyamic acid) nanofibres were obtained. The polyimide nanofibres have shown excellent mechanical properties in the form of mats based on our previous study [50]. This study shows that the single electrospun polyimide nanofibres had very high ultimate tensile strength up to 1.7 GPa and very high tensile modulus up to 76 GPa, compatible with those of their thicker-diameter counterparts with high chain alignment along the fibre axis [62–64]. X-ray diffraction and SEM/TEM-based fractography were further performed to examine the chain orientation and tensile failure mechanisms in these high-strength nanofibres. Finally, discussion and conclusions of this study are addressed.

2. Experimental

2.1. Preparation of polymer solution for electrospinning

The polymer solution used for electrospinning was prepared from poly(*p*-phenylene biphenyl tetracarboxamide acid) [polyamic acid (BPDA/PPA)], which was synthesized from 3,3',4,4'-biphenyltetracarboxylic dianhydride (BPDA, Hebei Jida Plastic Products Co., China) and *p*-phenylenediamine (PPA, Aldrich, USA) as reported in our previous study [50]. The intrinsic viscosity of the polyamic acid was $5.2\ \text{dl g}^{-1}$ at $25\ ^\circ\text{C}$ in *N,N*-dimethylacetamide (DMAc, Shanghai Jinwei Chemical Co., China). The number of the average molecular weight (M_w) was 2.7×10^5 , measured using a Waters 1515 system with a polystyrene standard for calibration. The

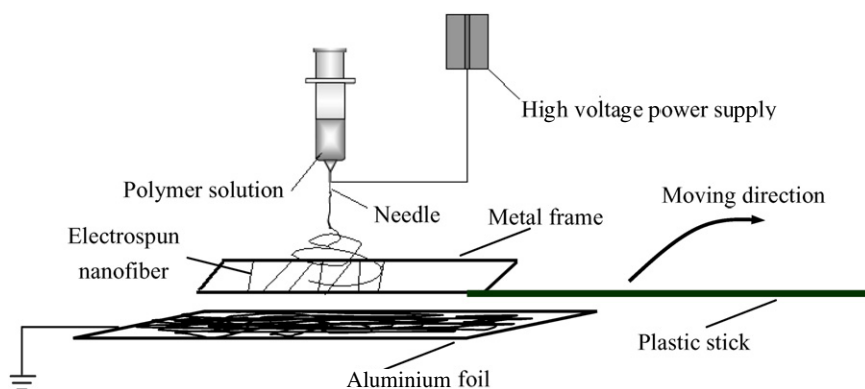


Figure 1. A schematic of collecting individual nanofibres on a metal frame.

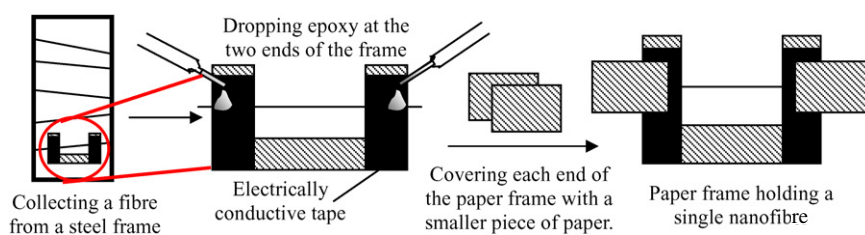


Figure 2. A schematic of carrying a single nanofibre on a paper frame.

polymer solution was prepared by dissolving the polyamic acid (3.0 wt%) and dodecyl ethyldimethylammonium bromide (DEMAB, Aldrich) (0.1 wt) in DMAc. The small quantity of DEMAB was added into the solution to increase the electrical conductivity of the solution.

2.2. Electrospinning of polyimide nanofibres and preparation of single nanofibre samples

The precursor (polyamic acid) nanofibres were produced by electrospinning based on the above polymer solution. A 50 kV electrical voltage was applied across a 25 cm gap between the spinneret and a grounded aluminium foil with an area of $200 \times 200 \text{ mm}^2$. The feeding rate of the solution was 2.5 ml h^{-1} . A stainless steel frame with a rectangular opening of $30 \times 150 \text{ mm}^2$ was utilized as nanofibre collector as illustrated in figure 1. The steel frame was mounted on a plastic handle for the purpose of electrical isolation. During the electrospinning process, widely whipping nanofibres, which might span the frame opening, were collected when the steel frame was passed rapidly through the gap between the spinneret and the grounded aluminium foil. Consequently, the polyamic acid nanofibres collected on the steel frame were imidized in a high-temperature furnace according to the following protocol: (1) holding at 100°C in vacuum for 2 h to remove the residual solvent, (2) heating at a rate of 10°C per minute and annealing at 200°C in vacuum for 15 min, (3) heating at a rate of 5°C per minute and annealing at 300°C in vacuum for 60 min to complete the imidization of the precursor nanofibres, and (4) heating at a rate of 2°C per minute and annealing at 430°C in vacuum for 30 min.

A single nanofibre sample for the tension test was prepared by using a thick paper frame with a width of a 15 mm and

a length of 25 mm. Two pieces of double-sided electrically conductive adhesive tape were placed on the paper frame as shown in figure 2. Under bright light together with a dark background, separated individual nanofibres on the steel frame were visible due to the light scattering through the nanofibres. The paper frame located beneath the steel frame was moved upwards to a targeted nanofibre until the nanofibre was attached to the two pieces of the adhesive tape on the paper frame. After that, two droplets of super glue (ethyl-2-cyanoacrylate) were placed on the nanofibre segment on both pieces of the adhesive tape to ensure the bonding strength between the nanofibre segment and the paper frame. Consequently, each end of the paper frame was covered with a piece of paper to avoid the adhesive tape sticking to the clamps of the tension tester, as illustrated in figure 2.

2.3. Tension tests of single electrospun nanofibres

Tension tests of single electrospun nanofibres were performed on a micro tensile testing machine, JQ03B (Powereach, Shanghai, China). The tension tester is made up of a micro-load sensor (19.6 mN – $0.50 \mu\text{N}$, Minebea Co., Ltd, Japan), a high-magnification optical microscope MS160 (WDK, Japan), a digital camera, software for data acquisition and processing and a computerized control system. The testing process consists of five steps illustrated in figures 2–4. The first step is to load the single nanofibre sample on the paper frame (figure 2). The second (figure 3) is to mount the paper frame carrying the single nanofibre sample into the clamps of the micro tension tester. The third is to cut the ‘rib’ of the paper frame. The fourth is to locate the nanofibre sample using the optical microscope to ensure that only one nanofibre sample is present (figure 4). The last is to load the

single nanofibre sample to break with the micro tension tester (figure 4). Displacement-control testing scheme was adopted in the tension tests of all single nanofibre samples in this study. A constant loading rate of 1 mm min⁻¹ was utilized in the entire tensile testing process.

3. Results and discussion

3.1. Preparation of polymer solution for electrospinning

Except for sulfuric acid, polyimide is insoluble in almost all organic and inorganic solvents. Therefore, the polyimide nanofibres had to be fabricated by electrospinning a solution of their precursor (polyamic acid) in DMAc. The curing process was then used to convert the precursor nanofibres into polyimide nanofibres. In order to produce high-strength polyimide nanofibres, a high molecular-weight precursor is desired. The precursor used to fabricate the polyimide nanofibres was synthesized with very high molecular weight as reported in our recent study [50]. The intrinsic viscosity and relative molecular weight of the as-synthesized polyamic acid are listed in table 1. The solution for electrospinning was prepared by diluting the reaction mixture (polyamic acid and DMAc) with DMAc to decrease the viscosity and by

adding a small amount of DEMAB to enhance the electrical conductivity of the solution. A higher electrical conductivity of the solution is helpful for producing bead-free nanofibres [7]. The physical properties of the solution used in electrospinning are listed in table 1.

3.2. Preparation of single nanofibre sample for tension

Special care should be taken to capture a single nanofibre and to mount it into the micro tension tester. The detailed procedure to operate and mount an individual nanofibre sample has been described in section 2.2. After each tension test, the broken fibre segments were used for the characterization of the nanofibre diameter by using SEM. Therefore, besides attaching the targeted nanofibre sample on the paper frame, the adhesive was also used to retain the ends of the nanofibre sample in the single fibre tension test.

3.3. Tension tests of single electrospun nanofibres

A micro tension test of single nanofibres is capable of providing complete information of the mechanical response of individual electrospun nanofibres subjected to axial tension. In this study, micro tension tests of single electrospun polyimide nanofibres and polyamic acid nanofibres were performed on the micro tension tester JQ03B. In each tension test, the single fibre sample carried on the paper frame could be translated feasibly and mounted into the clamps of the micro tension tester. The ‘rib’ of the paper frame was cut carefully, leaving the two ends attached to the clamps of the tester. With the aid of an intense light source, the location of the nanofibre can be detected under the optical microscope which was equipped with a digital camera (figure 4). Nevertheless, the nanofibre diameter can only be estimated under the equipped optical microscope since it was below the visible light wavelengths.

For the purpose of accurate measurement of the nanofibre diameter, the optical microscope was helpful for locating the fibre segment on the paper frame after the tension test. One of the broken fibre segments on the paper frame was marked under the optical microscope, cut out and coated with a thin gold layer (~3 nm) to prevent electrical charging within the SEM. The gold layer thickness was characterized using AFM

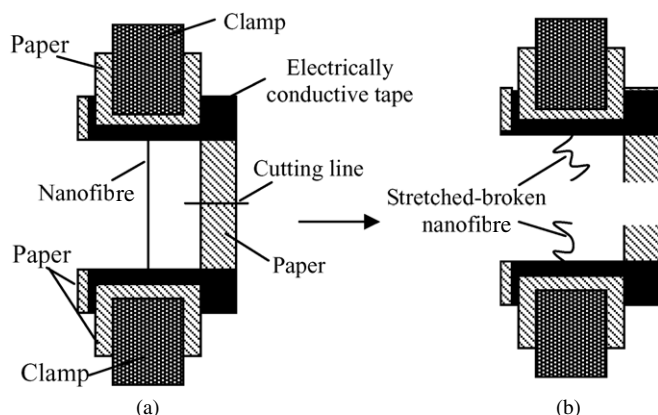


Figure 3. (a) A schematic diagram of the paper frame holding a single nanofibre into the clamps for tension test. (b) The paper frame was cut to let the nanofibre hang on the clamps of the micro tension tester and the single nanofibre was stretched until broken.

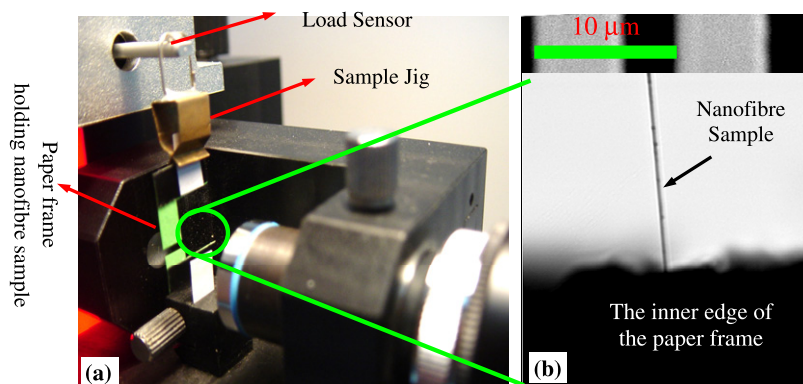


Figure 4. (a) The paper frame carrying a single nanofibre into the clamps of the testing machine. (b) An optical image showing the tensile stretching of a single nanofibre. The calibrated scale bar is shown at the top of (b).

Table 1. Properties of BP-PAA and the DMAc solution for electrospinning.

Sample No	$[\eta]$ (dL g^{-1})	Mw	Mn	Mw/Mn	Conc. of BPPAA (wt%)	Conc. of DEMAB (wt%)	Viscosity (Pa s)	Electrical conductivity ($\mu\text{S cm}^{-1}$)
1	5.2	5.1×10^5	2.7×10^5	1.9	3.0	0.1	6.08	57.0

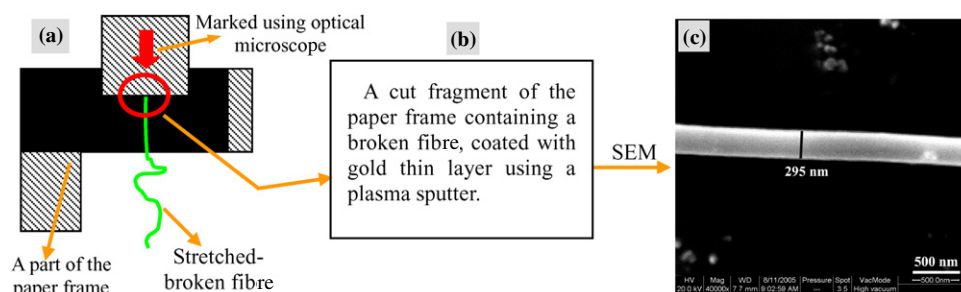


Figure 5. A schematic of the steps for determining the diameter of the applied single nanofibre. (a) A part of the paper frame containing a single broken nanofibre was marked using an optical microscope and cut. (b) The cut fragment of the marked part of the paper frame was coated with a gold thin layer using a plasma sputter. (c) A high-resolution SEM image used to determine the diameter of the stretched and broken single nanofibre.

(Micronano AFM-II/III 3000, Zhuolun MicroNano Co., Ltd, Shanghai, China) through scanning controlled gold patterns formed in the gold coating process. These patterns were created by using a mask placed on a mica sheet, which was located close to the fibre sample during the coating process. The diameter of gold-coated nanofibres was measured using SEM (Quanta 200, FEI, USA), as shown in figure 5.

The original fibre diameter before testing was used for calculating the ultimate tensile strength and axial tensile modulus based on the experimental force–displacement curves recorded in the tension tester. This fibre diameter was determined by measuring the diameter of the nanofibre segment out of the super glue droplet on the paper frame. Clearly, the fibre segment out of the super glue droplet was tension-free during the entire tension test and can be easily detected, marked and cut out for the SEM characterization. The thickness of the gold layer (~ 3 nm) was deducted from the fibre diameter. The gauge length of each tested fibre was measured between the edges of the adhesive tapes (~ 12 mm).

Typical stress–strain curves of single polyamic acid and polyimide nanofibres are plotted in figure 6. The experimental parameters and the mechanical properties of the single nanofibres extracted from figure 6 are summarized in table 2. It can be seen that the average ultimate tensile strength and axial tensile modulus of single polyamic acid nanofibres with diameter of around 300 nm are 766 ± 41 MPa and 13 ± 0.39 GPa, respectively. The corresponding average ultimate strain is up to 43%. However, for single polyimide nanofibres with similar diameter, the average ultimate tensile strength is increased up to 1.7 ± 0.12 GPa, and the axial tensile modulus is enhanced up to 76 ± 12.6 GPa. Correspondingly, the average ultimate strain is dropped to 3%.

It can be observed from figure 6(a) that the stress–strain curves of three typical polyamic acid nanofibre samples have very similar growth trends. This indicates the reliability of the present testing method. In addition, each stress–strain curve of polyamic acid is made of two nearly linear stress–strain stages. The first stage corresponds to the linearly elastic region similar

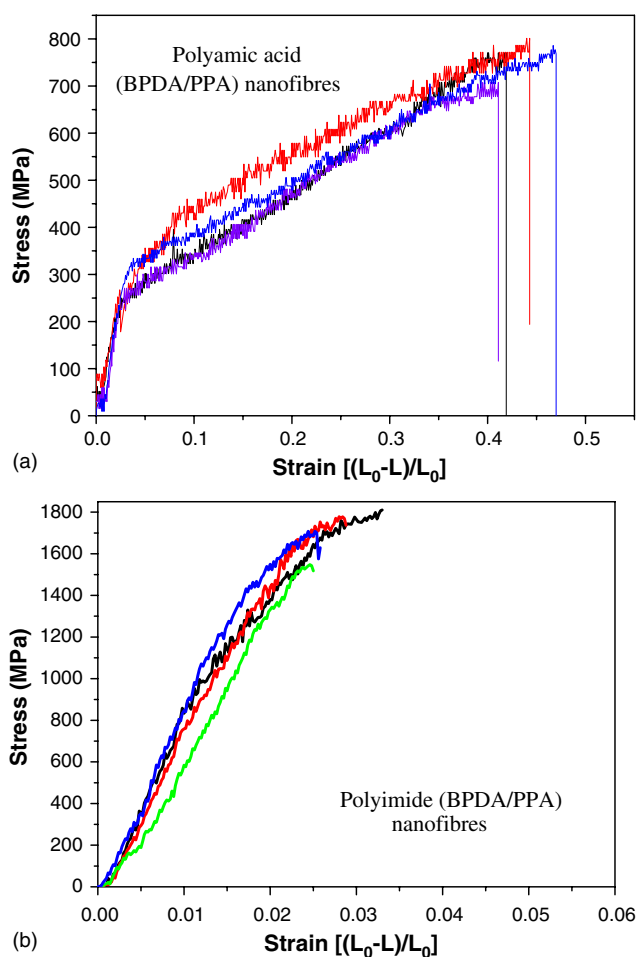
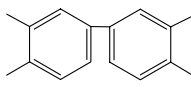


Figure 6. Typical stress–strain curves of single electrospun (a) polyamic acid nanofibres and (b) polyimide nanofibres.

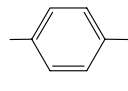
to that of most linearly elastic materials, and the second region corresponds to the linearly strain-hardening region with very large plastic deformation till the final breakage point at ultimate strain up to 43%. In the region, significant chain sliding

Table 2. Mechanical properties of single polyamic acid (BPDA/PPA), polyimide (BPDA/PPA) nanofibres and conventional polyimide fibres.

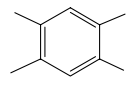
Sample no.	Diameter (nm)	Load force (μN)	Tensile strength (MPa)	Tensile modulus (GPa)	Percentage of elongation (%)	
Polyamic acid	1	221	30.1	786	13.5	46.7
	2	227	28.6	707	13.0	40.5
	3	250	39.3	801	13.9	44.3
	4	239	34.5	770	13.2	41.7
	Average			766 \pm 41	13 \pm 0.39	43.3 \pm 2.4
Polyimide	1	237	75.1	1703	89.3	2.6
	2	289	101.2	1544	59.6	2.5
	3	219	66.9	1776	75.3	2.8
	4	280	111.4	1810	81.8	3.3
	Average			1708 \pm 118	76 \pm 12.6	2.8 \pm 0.36
Conventional polyimide fibres	Repeating unit structure					
	BPDA/PPD* [62]		1250	86	0.9	
	BPDA/PMDA/OTOL** [63, 64]		3100	128	2.6	
	BPDA/PPD/PMR*** [62]		5100	282	2.8	



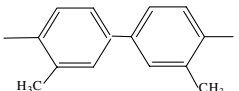
*BPDA



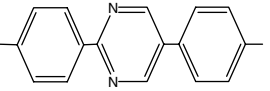
*PPD



*PMDA



**OTOL



***PMR

happened. The initial yield stress of this type of polyamic acid nanofibres can be determined from figure 6(a), which is around 250 MPa, and the corresponding initial yield strain is close to 5%. The present stress–strain curves (figure 6(a)) also indicate that polyamic acid nanofibre is a stable strain-hardening ductile material without a clear stress-softening phenomenon before its final failure.

The typical stress–strain curves of polyimide nanofibres are shown in figure 6(b). Again, the experimental curves indicated a very good reliability of the micro tensile testing method introduced in this study. In contrast to polyamic acid nanofibres above, the electrospun polyimide nanofibres with diameter \sim 300 nm behaved simply brittle when subjected to axial tension in the present tests. From figure 6, it can be clearly observed that after annealing the ultimate tensile strength and axial tensile modulus of polyimide nanofibres have been improved substantially. Specifically, the ultimate tensile strength was doubled and the axial tensile modulus was improved up to six times that before annealing. This remarkable improvement of the ultimate tensile strength and axial tensile modulus is due to the stiffening of microstructures of the polyimide nanofibres induced by the formation of new covalent chemical bonds during the annealing process. The high ultimate tensile strength and axial tensile modulus of the polyimide nanofibres are very close to the mechanical properties of their larger-diameter counterparts with highly

aligned macromolecular chains [62–64]. It is expected that the alignment of polyimide molecules along the fibre axis was formed during the electrospinning process.

3.4. X-ray diffraction of crystallization and TEM-fractographical analysis

Wide angle x-ray diffraction (WAXD) analysis was performed in examining the crystallization in the nanofibres (films made up of highly aligned nanofibre) considered in this study. The x-ray diffraction patterns are shown in figure 7, from which it can be observed that the rigid rod-like polyimide was partially crystalline. Curve *a* in figure 7 shows that the crystallites in a polyimide film (non-stretched and created by solution cast) were randomly distributed and therefore led to the WAXD patterns. If there were no polyimide molecular alignment in the nanofibres, the crystallites in the non-aligned nanofibre mat should also be randomly distributed, as those in the film. However, the WAXD patterns (curve *c* in figure 7) of the non-aligned nanofibre mat show that the peak (1 1 0) was magnified, while the (2 0 0) and (2 1 0) peaks were weakened by comparison with the intensity of those peaks from the polyimide film. This shows that the polyimide molecules in nanofibres were oriented along the axis of the small fibres. Furthermore, the curve *b* in figure 7 shows that the (1 1 0) peak is stronger while the (2 0 0) and (2 1 0) peaks are weaker and

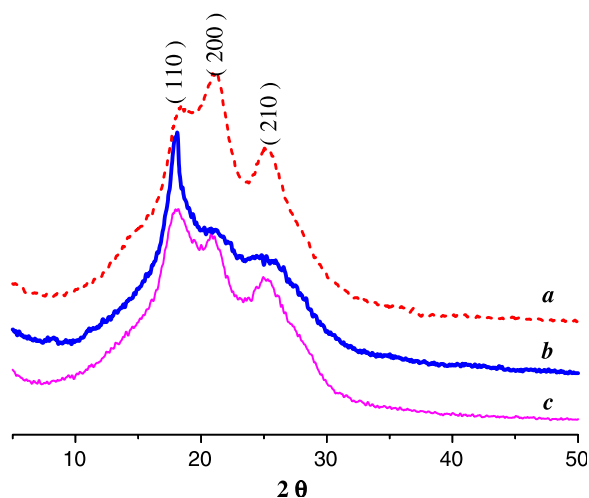


Figure 7. WAXD patterns of polyimide film and electrospun nanofibre mats cured at 430 °C: (a) polyimide film (18 μm thick); (b) multilayer aligned polyimide nanofibre mat and (c) multilayer non-aligned polyimide nanofibre mat.

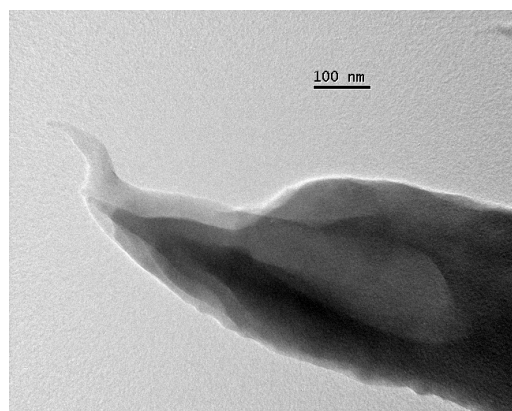
broader. As a matter of fact, both fibre alignment in the mat and molecular orientation in the fibre influence the WAXD patterns.

Consequently, by using a transmission electron microscope (JEOL JEM 2010 TEM, 200 kV, Japan), detailed fractographical analysis was performed to examine the failure mechanisms of polyimide nanofibres subjected to quasi-static axial tension. In fact, it was difficult to directly operate a single broken polyimide nanofibre within the TEM. Therefore, a bundle of polyimide nanofibres (a tiny unidirectional nanofibre film) was first gradually stretched to failure under the same loading rate as that used in single nanofibre tension tests, and then the failed nanofibre bundle was examined by using TEM. Images shown in figure 8 are the typical tensile failure modes of the polyimide nanofibres captured from the tips of failed nanofibres in the bundle. It is expected that the failure modes in single polyimide nanofibres would be very close to those in the bundle of polyimide nanofibres. From figure 8, it can be observed that the tensile failure of polyimide nanofibres is due to a brittle fracture and there is no clear necking near the fractured surfaces. Due to the very long polyimide chains up to $\sim 1 \mu\text{m}$, chain pull-out is clearly detected. The smooth fractured surfaces correspond to the chain scission and the breakage of the chain bundle.

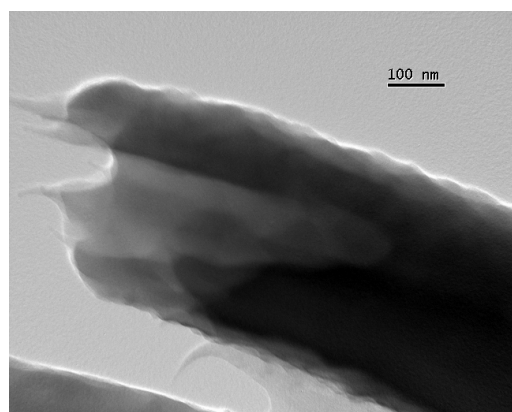
4. Conclusion

High-strength rigid-rod polyimide nanofibres with diameters below 300 nm have been produced successfully by annealing their precursor (polyimide acid) nanofibres that were fabricated by the electrospinning technique. Mechanical characterization of the precursor (polyamic acid) nanofibres and polyimide nanofibres has been performed successfully by the micro tension test introduced in this study.

This study has shown that electrospun polyamic acid nanofibres with diameter $\sim 300 \text{ nm}$ had an average tensile strength of $766 \pm 41 \text{ MPa}$, modulus of $13 \pm 0.39 \text{ GPa}$



(a)



(b)

Figure 8. TEM-fractographical analysis of polyimide nanofibres after tensile failure.

and ultimate strain $\sim 43\%$. After annealing the precursor (polyamic acid) nanofibres, the rigid-rod polyimide nanofibres exhibited excellent mechanical properties with an average tensile strength up to $1.7 \pm 0.12 \text{ GPa}$ and modulus of $76 \pm 12.6 \text{ GPa}$. However, the ultimate strain was decreased to $\sim 3\%$. The tensile properties of the polyimide nanofibres were close to those of the thicker conventional polyimide fibres with very high molecular weight and molecular alignment formed through stretching after extrusion. The experimental stress-strain curves show that the precursor polyamic acid nanofibres behaved like linearly strain-hardening ductile material without obvious softening at the final failure. However, after annealing, the polyimide nanofibres behaved as simply brittle material with much higher axial modulus and ultimate tensile strength while very lower ultimate strain compared with those of the polyamic acid nanofibres. The high tensile strength and axial modulus and low ultimate strain indicate that most of the long polyimide molecules have been aligned along the nanofibre axis during electrospinning that has been validated by the WAXD in this study. The failure mechanisms of the polyimide nanofibres subjected to quasi-static axial tension have also been examined by the TEM-based fractographical analysis of the failed nanofibre samples, which include chain scission, pull-out and bundle breakage, among others.

This study has reported the highest ultimate tensile strength and axial tensile modulus of electrospun nanofibres

among those reported in the literature to date. This study paves the way for developing ultrahigh-strength electrospun nanofibres for nanocomposites and nanofibre devices. The practicable testing method demonstrated in this study can also be used for the mechanical characterization of other nanofibres, nanotubes and nanowires.

Acknowledgments

Financial support was gratefully acknowledged from the National Natural Science Foundation of China (Grants 20464001 and 20674034), the Jiangxi Provincial Department of Science and Technology (Grant 050008: Jiangxi Provincial Main Discipline Academic & Technological Leader Project) and the National Science Foundation (NSF) of the USA (Grants DMI-0100354 and DMI-0403835).

References

- [1] Doshi J and Reneker D H 1995 *J. Electrostat.* **35** 151
- [2] Reneker D H and Chun I 1996 *Nanotechnology* **7** 216
- [3] Dzenis Y 2004 *Science* **304** 1917
- [4] Li D and Xia Y N 2004 *Adv. Mater.* **16** 1151
- [5] Reneker D H, Yarin A L, Zussman E and Xu H 2007 *Adv. Appl. Mech.* **41** 43
- [6] Greiner A and Wendorff J H 2007 *Angew. Chem. Int. Ed.* **46** 5670
- [7] Huang C B, Chen S L, Lai C L, Reneker D H, Qiu H, Ye Y and Hou H Q 2006 *Nanotechnology* **17** 1558
- [8] Zhang Y Z, Venugopal J, Huang Z M, Lim C T and Ramakrishna S 2006 *Polymer* **47** 2911
- [9] Tan S H, Inai R, Kotaki M and Ramakrishna S 2005 *Polymer* **46** 6128
- [10] Allcock H R, Steely L B and Singh A 2006 *Polym. Int.* **55** 621
- [11] Acatay K, Simsek E, Ow-Yang C and Menciloglu Y Z 2004 *Angew. Chem. Int. Ed.* **43** 5210
- [12] Yuan X Y, Zhang Y Y, Dong C H and Sheng J 2004 *Polym. Int.* **53** 1704
- [13] Miyoshi T, Toyohara K and Minematsu H 2005 *Polym. Int.* **54** 1187
- [14] Teo W E and Ramakrishna S 2006 *Nanotechnology* **17** R89
- [15] Gibson P, Schreuder-Gibson H and Rivin D 2001 *Colloids Surf. A—Physicochem. Eng. Asp.* **187** 469
- [16] Huang Z M, Zhang Y Z, Kotaki M and Ramakrishna S 2003 *Compos. Sci. Technol.* **63** 2223
- [17] Bognitzki M, Hou H Q, Ishaque M, Frese T, Hellwig M, Schwarte C, Schaper A, Wendorff J H and Greiner A 2000 *Adv. Mater.* **12** 637
- [18] Liu W X, Graham M, Evans E A and Reneker D H 2002 *J. Mater. Res.* **17** 3206
- [19] Sutasinpromprae J, Jitjaicham S, Nithitanakul M, Meechaisue C and Supaphol P 2006 *Polym. Int.* **55** 825
- [20] Yang K S, Edie D D, Lim D Y, Kim Y M and Cho Y O 2003 *Carbon* **41** 2039
- [21] Kim J S and Reneker D H 1999 *Polym. Compos.* **20** 124
- [22] Smith D, Reneker D H, Kataphinan W and Dabney A 2001 *PCT Int. Appl. WO 2000-US27775*
- [23] Smith D and Reneker D H 2001 *PCT Int. Appl. WO 2000-US27776*
- [24] Li W J, Laurencin C T, Catterson E J, Tuan R S and Ko F K 2002 *J. Biomed. Mater. Res.* **60** 613
- [25] Matthews J A, Wnek G E, Simpson D G and Bowlin G L 2002 *Biomacromolecules* **3** 232
- [26] Burger C, Hsiao B S and Chu B 2006 *Annu. Rev. Mater. Res.* **36** 333
- [27] Kenawy E R, Bowlin G L, Mansfield K, Layman J, Simpson D G, Sanders E H and Wnek G E 2002 *J. Control. Release* **81** 57
- [28] Chew S Y, Wen Y, Dzenis Y and Leong K W 2006 *Curr. Pharm. Des.* **12** 4751
- [29] Onozuka K, Ding B, Tsuge Y, Naka T, Yamazaki M, Sugi S, Ohno S, Yoshikawa M and Shiratori S 2006 *Nanotechnology* **17** 1026
- [30] Song M Y, Kim D K, Ihn K J, Jo S M and Kim D Y 2004 *Nanotechnology* **15** 1861
- [31] Jiang L, Zhao Y and Zhai J 2004 *Angew. Chem. Int. Ed.* **43** 4338
- [32] Miyauchi Y, Ding B and Shiratori S 2006 *Nanotechnology* **17** 5151
- [33] Ding B, Kim J H, Miyazaki Y and Shiratori S M 2004 *Sensors Actuators B—Chem.* **101** 373
- [34] Norris I D, Shaker M M, Ko F K and MacDiarmid A G 2000 *Synth. Met.* **114**, 109
- [35] Wu X F and Dzenis Y A 2005 *J. Appl. Phys.* **98** 093501
- [36] Wu X F and Dzenis Y A 2006 *J. Appl. Phys.* **100** 124318
- [37] Wu X F and Dzenis Y A 2007 *J. Appl. Phys.* **102** 044306
- [38] Wu X F and Dzenis Y A 2007 *Nanotechnology* **18** 285702
- [39] Wu X F and Dzenis Y A 2007 *J. Phys. D: Appl. Phys.* **40** 4276
- [40] Chatterjee A P 2006 *J. Appl. Phys.* **100** 054302
- [41] Chatterjee A P and Prokhorova D A 2007 *J. Appl. Phys.* **101** 104301
- [42] Bobaru F 2007 *Model. Simul. Mater. Sci. Eng.* **15** 397
- [43] Lee K H, Kim H Y, La Y M, Lee D R and Sung N H 2002 *J. Polym. Sci. B: Polym. Phys.* **40** 2259
- [44] Hansen L M, Smith D J, Reneker D H and Kataphinan W 2005 *J. Appl. Polym. Sci.* **95** 427
- [45] Lee K H, Kim H Y, Khil M S, Ra Y M and Lee D R 2003 *Polymer* **44** 1287
- [46] Lee K H, Kim H Y, Ryu Y J, Kim K W and Choi S W 2003 *J. Polym. Sci. B: Polym. Phys.* **41** 1256
- [47] Nair L S, Bhattacharyya S, Bender J D, Greish Y E, Brown P W, Allcock H R and Laurencin C T 2004 *Biomacromolecules* **5** 2212
- [48] Hou H Q, Ge J J, Zeng J, Li Q, Reneker D H, Greiner A and Cheng S Z D 2005 *Chem. Mater.* **17** 967
- [49] Ayutsede J, Gandhi M, Sukigara S, Micklus M, Chen H E and Ko F 2005 *Polymer* **46** 1625
- [50] Huang C B, Chen S L, Reneker D H, Lai C L and Hou H Q 2006 *Adv. Mater.* **18** 668
- [51] Tan E P S and Lim C T 2004 *Appl. Phys. Lett.* **84** 1603
- [52] Tan E P S and Lim C T 2004 *Rev. Sci. Instrum.* **75** 2581
- [53] Wang M, Jin H J, Kaplan D L and Rutledge G C 2004 *Macromolecules* **37** 6856
- [54] Guhados G, Wan W K and Hutter J L 2005 *Langmuir* **21** 6642
- [55] Gu S Y, Wu Q L, Ren J and Vancso G J 2005 *Macromol. Rapid Commun.* **26** 716
- [56] Tan E P S, Ng S Y and Lim C T 2005 *Biomaterials* **26** 1453
- [57] Tan E P S, Goh C N, Sow C H and Lim C T 2007 *Appl. Phys. Lett.* **86** 073115
- [58] Inai R, Kotaki M and Ramakrishna S 2005 *Nanotechnology* **16** 208
- [59] Tan E P S and Lim C T 2006 *Compos. Sci. Technol.* **66** 1102
- [60] Zussman E, Burman M, Yarin A L, Khalifin R and Cohen Y 2006 *J. Polym. Sci. B: Polym. Phys.* **44** 1482
- [61] Tan E P S, Ng S Y and Lim C T 2005 *Biomaterials* **26** 1453
- [62] Mihailov G M, Korzawin L N, Lebejeva M F and Baklagina Y G 1998 *J. Pract. Chem. (Russ)* **71** 2040
- [63] Kaneda T, Katsura T, Kanji N, Makino H and Horio M 1986 *J. Appl. Polym. Sci.* **32** 3133
- [64] Kaneda T, Katsura T, Kanji N, Makino H and Horio M 1986 *J. Appl. Polym. Sci.* **32** 3151